Eur. J. Mech., B/Fluids, **10**, n° 2 - Suppl., 253-260, 1991

Wavelength selection and transients in the one-dimensional array of cells of the printer's instability

M. RABAUD, Y. COUDER and S. MICHALLAND

Laboratoire de Physique Statistique de l'École Normale Supérieure,
24, rue Lhomond, 75231 Paris Cedex 05, France

Abstract. The printer's instability can provide a large array of identical cells. In the present article we show that for a given value of the control parameter, the wavelength is strictly selected. We investigate various processes (parity-breaking waves, Eckhaus-like instability, spatiotemporal dislocation) by which the pattern changes wavelength after a jump of this control parameter.

1. Introduction

Unbound front instabilities lead to pattern formation as dendritic growth or viscous fingering (Mullins and Sekerka [1964] and Saffman and Taylor [1958]). When bound by a gradient, however, a mean linear front can be stabilized. It destabilizes to form a series of cells. These fronts form an excellent tool for the investigation of the dynamical regimes of one dimensional extended systems. Such is the case in directionnal solidification (recents works can be found in de Cheveigné et al. [1986] and Bechhoefer et al. [1989]) and in the printer's instability ([Hakim et al., 1988], [Couder et al., 1989], [Rabaud and Hakim, 1989], [Rabaud et al., 1990]). This latter instability affects the meniscus of a viscous fluid placed between two moving non parallel solid surfaces. It occurs in several industrial film coating processes where it is often called the ribbing or the coating instability. For this reason it is mainly the instability threshold which was investigated initially (e.g. Taylor [1963], Savage [1977], Ruschak [1985] and Coyle et al. [1990]). Revisiting this type of instability we showed that the two surface velocities form two independant control parameters and that many different dynamical regimes could be observed in this system.

We first rapidly present the experimental apparatus in part 2. We study the permanent states and the wavelength selection in part 3. Transients associated with the increase or the decrease of the control parameter will be presented in part 4.

2. Experimental Set-Up

The cell is formed by two horizontal glass cylinders (L_i = 380 mm and L_o = 420 mm long) of different radii ($R_i = 33 \pm 0.01$ mm and $R_o = 50 \pm 0.05$ mm) one inside the other. They are off-centered (Fig. 1) so that there is a small gap on one generatrix, at the bottom of the apparatus ($0.1 < b_o < 1$ mm). The two cylinders can rotate independently and a small amount of silicon oil (Rhodorsyl 47V100) introduced between them, fills the gap.

For low velocities of the cylinders we observe from below two linear and parallel dark lines. These dark lines represent menisci limiting the domain where the gap is completely filled by oil (as the oil wets completely the glass cylinders, there are two coating films of oil on the moving surfaces). For larger velocities, one of the

0997-7546/91/ 253 8/$ 2.80/

two interfaces becomes wavy. Essentially, the instability is unaffected by the exact quantity of oil, provided there is enough oil to fill in the gap. The two air-oil interfaces are observed from below, through the outer cylinder, by a CCD video camera. Video pictures can be digitized and analyzed on a Macintosh IIx computer. In particular we can choose one single video-line that intercepts all the cells of the pattern, and digitize and memorize this line with a given time step. By collecting all these lines we reconstruct spatiotemporal images of the interface evolution that are powerful tools for understanding the temporal dynamics of the pattern.

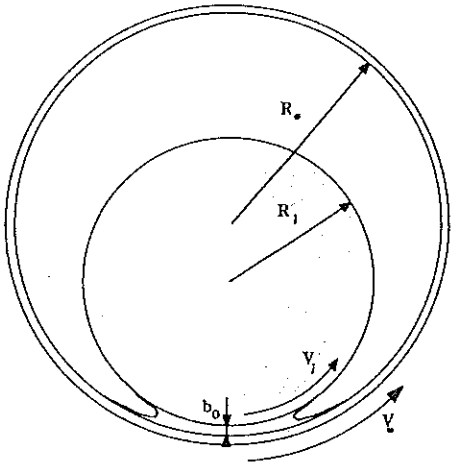

Figure 1 : Sketch of the experimental apparatus showing the two rotating cylinders coated by oil and the two menisci limiting the gap region.

3. Permanent States and their Wavelength Selections

In the case where the two cylinders rotate, the experiment reveals various dynamical regimes of the interface. States of travelling cells or of intermittent chaos can be studied [R. & al., 1990]. But, in the present work we restrict ourself to the wavelength selection problem when only one cylinder rotates and to the transient behaviours. In this situation, for a given value of the parameters, there is only one final state which is stationary in the laboratory frame of reference. As the rotation of the inner or outer cylinder have identical effects on the interface, we choose to rotate the inner one as its mechanical properties are better defined (± 0.01 mm on the radius and all along the cylinder).

Starting from no rotation and increasing the velocity of this cylinder, at a given onset, the front becomes a sinusoid of wavelength λ_c. This instability is clearly supercritical ; there is no hysteresis, zero amplitude at onset and close to V_c the amplitude increases as $(V - V_c)^{0.5}$. We wrote a linear analysis when only one cylinder is rotating [H. & al., 1988] and emphasized a strong analogy with the equations of directional growth of a crystal [R. & H., 1989]. This linear analysis gives correct predictions for the values of λ_c and for the critical velocity at onset, it is also in qualitative agreement with the analysis of Savage [1977] and with the computation of Coyle *et al.* [1990]. This analysis shows that the relevant parameters are the capillary number $Ca = \mu V/T$ (where μ and T are dynamical viscosity and surface tension of the oil and V the tangential velocity of the moving cylinder) and the ratio b_0/R of the gap thickness to its radius of curvature in the gap region ($R = R_i R_o / (R_o - R_i)$).

At onset, in our range of geometrical parameters ($0.1 \leq b_0 \leq 2$ mm, $10 \leq R \leq 100$ mm), typical critical values are :

$$Ca_c \approx 40 \frac{b_0}{R} \quad \text{and} \quad \lambda_c \approx 4\sqrt{b_0 R}.$$

As in directional growth experiments, a dimensionless parameter, the Péclet number, ratio of the wavelength of the pattern to the characteristic length scale of the pressure field. At onset we find $Pé_c \approx 10$.

When the speed of the cylinder increases the amplitude of the deformation grows, the front departs from its

sinusoidal shape and the wavelength λ of the pattern decreases (e.g. starting with 20 cells at onset we can have 100 at larger velocity). As the nonlinearity increases, the front becomes a series of parallel fingers separated by thin oil walls and the inward/outward symmetry is broken (Fig. 2). Above threshold, as the Péclet number decreases and becomes less than one, fingers shape becomes identical to the shape of wide Saffman-Taylor fingers [R. & H., 1989].

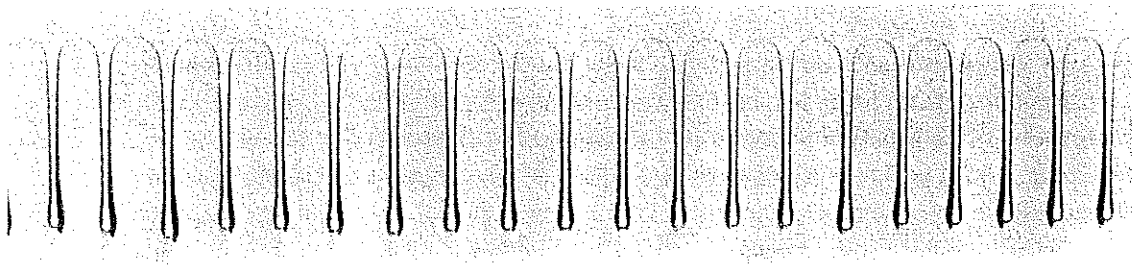

Figure 2 : Photograph of a stable pattern of stationary cells ($Ca \approx 10\, Ca_c$, $Pé \approx 1$).

For all velocity values, after long transients described in the next paragraphs, the pattern adapts to take an optimum wavelength without any defect. Provided the structure has sufficient time to evolve, there is no measurable hysteresis in the wavenumber versus velocity curve (Fig. 3).

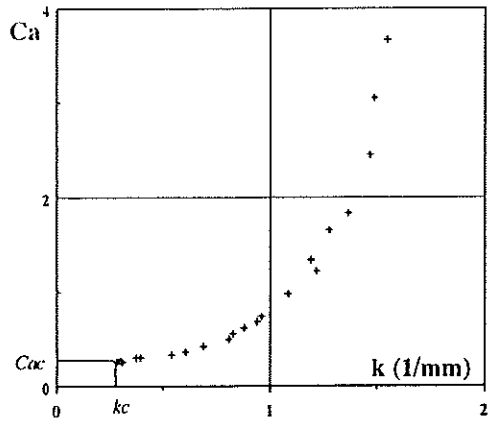

Figure 3 : Evolution of the selected wavenumber depending on the capillary number (b_0 = 0.46 mm).

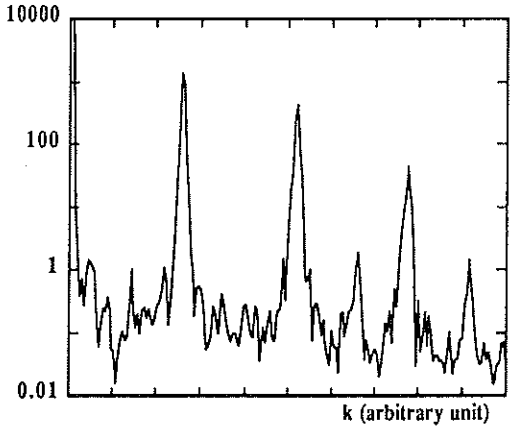

Figure 4 : Logarithm of the spatial power spectrum of a video-line intersecting a pattern of 50 cells.

The dispersion of the pattern can be determined by spatial Fourier transform (Fig. 4). For an interface of more than 50 cells, the width of the fundamental gives a wavenumber dispersion Δk/k of about 4% which is of the order of the numerical dispersion induced by the apodisation technic of the Fast Fourier Transform algorithm. (As the selected wavenumber evolves rapidly with the distance to threshold, the fluctuations in the gap thickness ($\Delta b_0 \approx 0.05$ mm) along the axis of the outer cylinder would also be sufficient to explain this dispersion of 4%.). Anyway, this dispersion is quite small and one order lower than in directional growth experiments [B. & *al.*, 1989], [de C. & *al.*, 1986].

There is no apparent discretization effects on the selected wavenumber, and indeed, at the extremities of the interface our boundary conditions are not rigid, there is no phase pinning. Near the ends of the cylinders two recirculations of oil usually affect the instability over one or two wavelengths, giving a rather free boundary condition. These end recirculations can be avoided when only a very small amount of oil is present in the

apparatus, so that the oil fills in the gap only in a central area. The instability then still occurs in the oil patch and with an homogeneous amplitude. This proves that the onset is not determined by end effects and that the bifurcation is not imperfect as suggested by Coyle *et al.* [1990] or as it is the case in Taylor-Couette experiments.

4. Transients

Transients to reach a new wavelength are different in duration and in behaviour for positive velocity jumps (where the pattern goes to shorter wavelengths) and negative velocity jumps (where it goes to larger wavelengths). Permanent states are reached in a shorter time for increasing velocity than for decreasing one.

Transients duration can be as long as thousands of rotation time of the moving cylinder. Qualitatively, this time increases with the length of the cylinders, the numbers of cells and with the decrease of the gap b_0. This evolution time (e.g. 20 mn) is of the order of the viscous diffusion time along the interface length L^2/ν although wavelength adaptation is not simply a diffusive process. Such long transients also exist in directional solidification and, as the pulling lengths are limited, the limited duration of these experiments can possibly explain the apparently weak wavelength selection.

4.1 Transients for Positive Velocity Jumps

In case of positive velocity jumps two main processes are observed depending on the shape of the fingers. This shape can be characterized by the ratio Γ of the depth over the width of each cells. In experimental conditions where the thickness gradient of the apparatus is small, Γ is small near onset and increases away from it. If the thickness gradient is large (e.g. experiments with one cylinder rotating over a stationary glass plate), Γ remains always small. The first process, in which parity-breaking waves propagate along the front, is only observed for small Γ. The second one, in which metastable large cells are created, can exist for all Γ but becomes the dominant process for cells of large Γ.

4.1.1. Parity breaking Waves

In the case of small positive velocity changes, and small Γ, a very typical process occurs (Fig. 5).

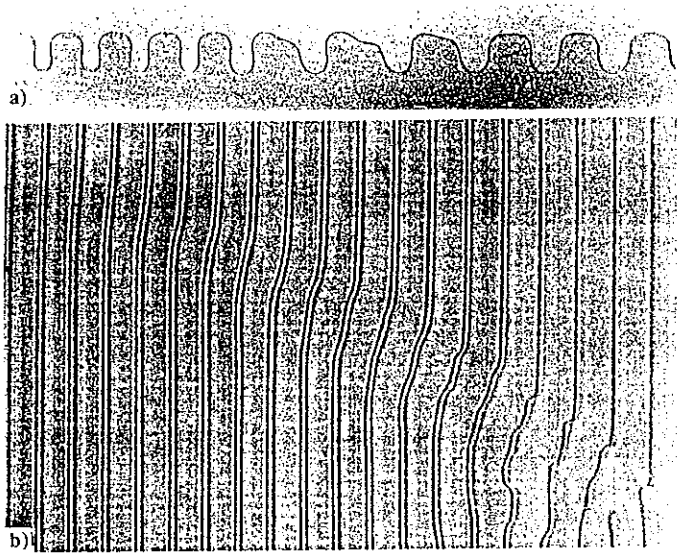

Figure 5 : (a) Photograph of an interface affected by a parity-breaking wave, (b) time evolution showing the propagation of this wave and the associated changes of wavelength. (Time elapses from top to bottom in 14 s.).

The one dimensional array of cells has to evolve from an initial wavelength λ_i to a shorter wavelength λ_f. The seed of the transformation is usually provided by one end of the interface (to the left on figure 5b). From this germ a wave propagates and spreads. Ahead of the wave the pattern is unchanged (wavelength λ_i), behind it the cells have their final stable wavelength λ_f. In-between, a few asymmetric cells drift in opposite direction from their envelope (phase velocity and group velocity are of opposite sign). The left and right borders of this wave have constant but different velocities. The wave packet width increases until an abrupt reduction by nucleation of a new cell. The wave of reduced width keeps propagating and the process repeats itself until reaching the extremity of the interface or colliding another parity-breaking wave. Similar propagative process have been observed in one dimensional array of cells of directional growth of eutectic by Cline [1984] and Faivre *et al.* [1989] and of liquid crystal by Bechhoefer *et al.* [1989]. A theoretical description has been presented by Coullet *et al.* [1989].

For larger velocity jumps, or starting from an imperfectly regular state, the situation is more complex as various germs exist and different waves propagate and interact.

4.1.2. Anomalous Cells

A different process is also observed which is the characteristic transient for deep cells (of large Γ of the type shown on Fig. 2). After the velocity jump at time t_0 (Fig. 6), various domains of original wavelength λ_i start to compress to their new smaller wavelength λ_f. As at first there is conservation of the number of cells, these domains are progressively separated by defects of increasing size. On figure 6, five such structures appear progressively. The two cells forming the defect become wider and asymmetrical (Fig. 7a, first picture). We call these localized states formed of two adjacent cells, anomalous cells. These cells are stable when their width is smaller than $3\lambda_f$. For larger width, they are unstable. The flattened part of their tip presents a side branching instability, an oscillation of the inner wall grows with increasing frequency and amplitude until one side branching succeeds in creating a new cell (Fig. 7a and b). The two anomalous cells break then into three cells of wavelength about λ_f.

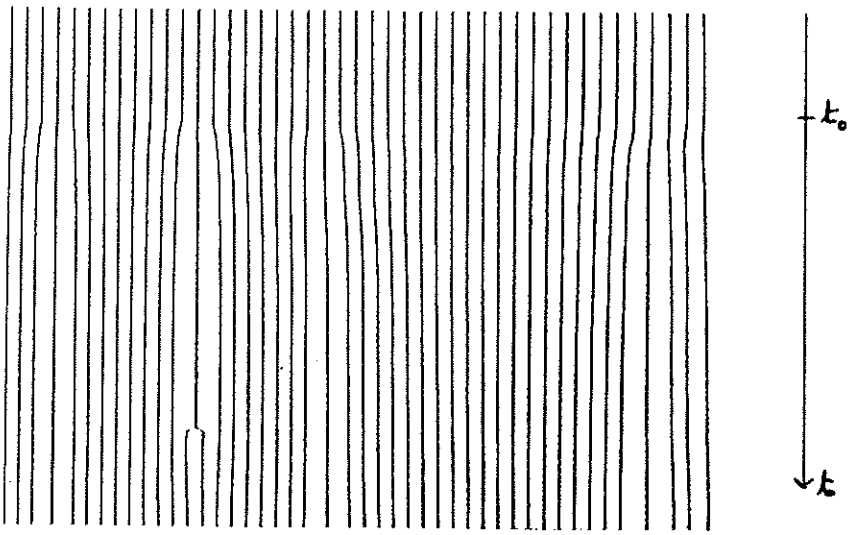

Figure 6 : Time evolution (from top to bottom in 75 s.) showing the birth of anomalous cells and the death of one. (Initially $Ca/Ca_c \approx 4.5$ and the jump correspond to a 7% change in wavenumber).

In time, all the anomalous cells will die and the pattern will end very regular with wavelength λ_f. As each anomalous cells is stationary in time and will nucleate one new cell, the mean distance W between these defects

is related to the wavelength change (Fig. 6). As n cells of size λ_i give (n+1) of size λ_f,

$$W = n\,\lambda_i = (n+1)\,\lambda_f = \frac{\lambda_i \lambda_f}{\lambda_i - \lambda_f}.$$

In this process, the initial wavelength becomes unstable after the velocity jump and a mode of long wavelength grows. This transient is similar to visualizations of Lowe and Gollub [1985] of the Eckhaus instability. Here we are far from onset and we must suppose that in the plane (Ca,k) of figure 3, one of the Eckhaus lines lie near and above of the experimental selection line. This could be the case, as shown numerically by Brattkus and Misbah [1990] for directional growth of a liquid crystal.

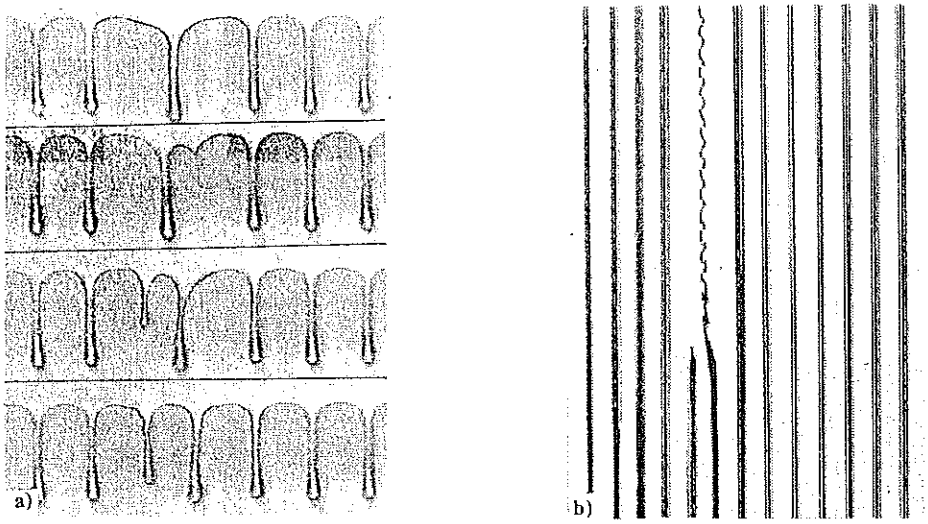

Figure 7 : (a) Successive photographs of an anomalous cell (time delay between pictures is 1.6 s.) showing the growth of the side-branching instability, (b) time evolution showing the death of this unstable structure (time elapses from top to bottom in 15 s.).

4.1.3. Halving of the Wavelength

Cases of fast adaptation to the new wavelength for particular values of the positive velocity jumps are also possible. Starting from a regular pattern of wavelength λ_i, we jump directly to a velocity where the stable state is $\lambda_f = \lambda_i/2$. In that case (Fig. 8) all the cells tip-split simultaneously. The time evolution is presented on figure 9, it shows that the system adapts in about 2 seconds to the new forcing. The same rapid transition have been observed for $\lambda_f = \lambda_i/3$.

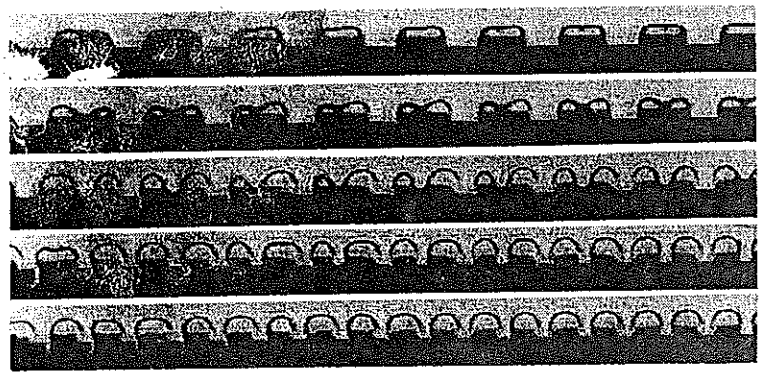

Figure 8 : Series of five successive pictures of the interface during the halving process.

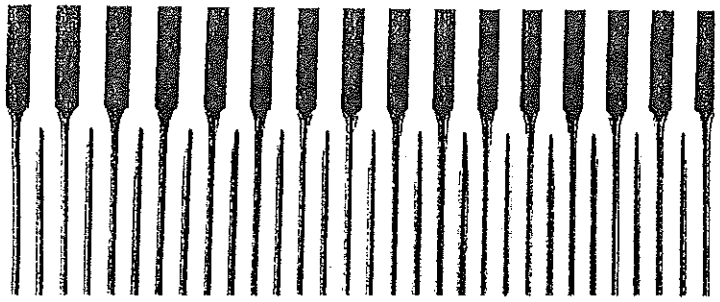

Figure 9 : Time evolution (from top to bottom in 15 s.) of one video-line during halving process .

4.2. Transients for Negative Velocity Jumps

The dynamics of transients for negative velocity jumps is different. After a small jump, nothing can happen for long times, suggesting that hysteresis does exist. But then, suddenly without visible precursor, one cell shrinks, decreases in amplitude and disappears. The adjacent cells increase in size and the pattern regularizes itself by a diffusion-like process. In the time evolution shown on figure 10, this looks like a spatiotemporal dislocation. But, unlike in dislocation in two dimensional array of rolls, there is here an asymmetry as the wavelength evolve in time.

For larger velocity jumps, various dislocations appears simultaneously along the interface. An equivalent of the parity-breaking wave phenomena can exist for decreasing velocity (the wave does not spread but shrinks) but it is only observed when starting from a non regular interface. The same process of rapid adaptation to the constraint is possible when adjusting the final state to be $\lambda_f = 2\lambda_i$, but the shrinking of one cell out of two is never perfectly synchronized all along the pattern.

The difference in the transient processes between an increase and a decrease of the forcing can be ascribed to the difference between the process of nucleation of a cell (by tip-splitting or side branching instability) and the annihilation process (by screening off of a cell in the pressure field) and so to the asymmetry between the tip and the walls of the cells.

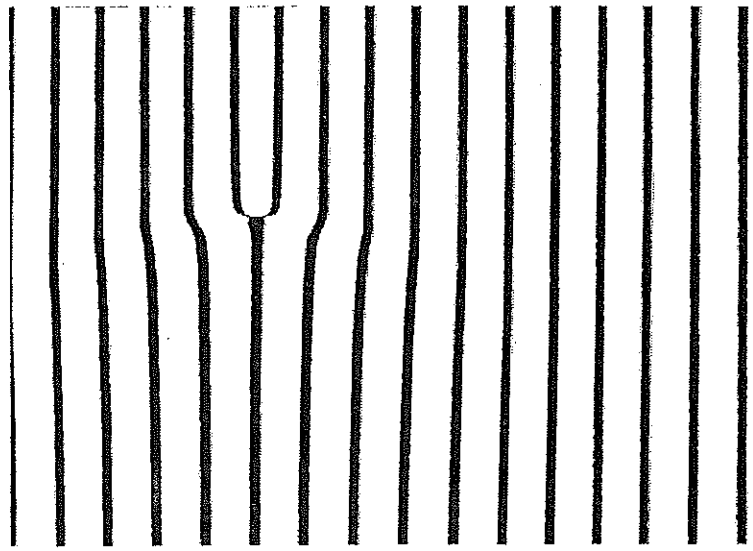

Figure 10 : Time evolution of one video-line (from top to bottom in 55 s.) during the lose of one cell.

5. Conclusion

We have shown that there is a very sharp wavelength selection in the array of cells formed by the printer instability. We have investigated the transient regimes by which a pattern adapts its wavelength to a change of the control parameter. For a decrease of the wavelength, the rearrangement of cells of small depth is fast due to the propagation of parity-breaking waves. This process is inhibited for cells of large depth. Their adaptation is slower ; intermediate metastable defects (anomalous cells) are formed. For an increase of the wavelength, localized annihilation, followed by a slow diffusion of phase, is observed.

The interest of these observations is two-fold. Firstly it is relevant to the discussion of the processes at work in other one-dimensional cellular patterns. Our results are a strong hint that parity-breaking waves are observed in liquid crystal directional phase transition [Bechhoefer *et al.* (1989)] and in eutectic directional growth [Faivre *et al.* (1989)] because the cells are shallow (small Γ) while they are inhibited in crystal directional solidification [de Cheveigné *et al.* (1986)] because the cells are deep (large Γ). Secondly the three processes that we observe here as transients forced by a velocity jump, occur spontaneously as local events in the chaotic regime (when the other cylinder is rotating).

Acknowledgment : We want to thank H. Thomé for continuous help during this experiment, and V. Croquette and V. Hakim for stimulating discussions.

Bechhoefer J., Simon A., Libchaber A. and Oswald P. (1989) Phys. Rev. A **40**, 2042.

Brattkus K. and Misbah C. (1990) Phys. Rev. Lett. **64**, 1935.

de Cheveigné S., Guthmann C. and Lebrun M.M. (1986) J. Phys. (Paris) **47**, 2095.

Cline H.E. (1984) Metallurgical Transactions **15**, 1013.

Couder Y., Michalland S., Rabaud M. and Thomé H., to appear in the proceedings of Nato Advanced Research Workshop, (Streitberg, September 1989) "Nonlinear Evolution of Spatio-Temporal Structures in Dissipative Continuous Systems", editors F.H. Busse and L. Kramer.

Coullet P., Goldstein R.E. and Gunaratne G.H. (1989) Phys. Rev. Lett. **63**, 1954.

Coyle D.J., Macosko C.W. and Scriven L.E. (1990) J. of Fluid Mech. **216**, 437.

Faivre G., de Cheveigné S., Guthmann C. and Kurowsky P. (1989) Europhys. Lett. **9**, 779.

Hakim V., Rabaud M., Thomé H. and Couder Y., to appear in the proceedings of Nato Advanced Research Workshop, (Cargèse 1988) "New Trends In Nonlinear Dynamics and Pattern Forming Phenomena : The Geometry of Nonequilibrium", editors P. Coullet and P. Huerre.

Lowe M. and Gollub J.P. (1985) Phys. Rev. Lett. **55**, 2575.

Mullins W.W. and Sekerka R.F. (1964) J. of Appl. Phys. **35**, 444.

Rabaud M. and Hakim V., to appear in the proceedings of "3rd International Workshop on Instabilities and Nonequilibrium Structures", (Valparaiso, Chili 1989), editors E. Tirapegui and W. Zeller, Kluwer Academic Publishers.

Rabaud M., Michalland S. and Couder Y. (1990) Phys. Rev. Lett. **64**, 184.

Ruschak K.J. (1985) Ann. Rev. Fluid Mech. **17**, 65.

Saffman P.G. and Taylor G.I. (1958) Proc. Roy. Soc. London, A **245**, 312.

Savage M.D. (1977) J. of Fluid Mech. **80**, 743.

Taylor G.I. (1963) J. of Fluid Mech. **16**, 595.